Cardiovascular Research (2015) **108**, 62–73
doi:10.1093/cvr/cvv208

Human epicardial adipose tissue has a specific transcriptomic signature depending on its anatomical peri-atrial, peri-ventricular, or peri-coronary location

Bénédicte Gaborit[1,2,3,4], Nicolas Venteclef[1,2,5], Patricia Ancel[1,2,3,4], Véronique Pelloux[1,2,3], Vlad Gariboldi[6], Pascal Leprince[1,2,7], Julien Amour[1,2,7], Stéphane N. Hatem[1,2,3,7], Elisabeth Jouve[8], Anne Dutour[4†*], and Karine Clément[1,2,3†*]

[1]Institute of Cardiometabolism and Nutrition, ICAN, Heart and Nutrition Department, Assistance-Publique Hôpitaux de Paris, Pitié-Salpêtrière Hospital, Paris F-75013, France; [2]Sorbonne Universities, University Pierre et Marie Curie-Paris 6, UMRS 1166, Paris F-75006, France; [3]INSERM, Nutriomics (team6 and Team3), UMR_S U1166, Paris F-75013, France; [4]Aix-Marseille Université, Faculté de Médecine, Department 'Nutrition, Obésité et Risque Thrombotique', INSERM, UMR 1062, INRA 1260, 13385 Marseille, France; [5]INSERM, UMRS_S1138, Paris F-75006, France; [6]Assistance-Publique Hôpitaux de Marseille, Cardiac Surgery, La Timone Hospital,13005 Marseille, France; [7]Assistance-Publique Hôpitaux de Paris, Pitié-Salpêtrière Hospital, Heart Department, 73013 Paris, France; and [8]Assistance-Publique Hôpitaux de Marseille, Medical Evaluation Department, CIC-CPCET, 13005 Marseille, France

Received 6 January 2015; revised 9 July 2015; accepted 23 July 2015; online publish-ahead-of-print 3 August 2015

Time for primary review: 54 days

Aims Human epicardial adipose tissue (EAT) is a visceral and perivascular fat that has been shown to act locally on myocardium, atria, and coronary arteries. Its abundance has been linked to coronary artery disease (CAD) and atrial fibrillation. However, its physiological function remains highly debated. The aim of this study was to determine a specific EAT transcriptomic signature, depending on its anatomical peri-atrial (PA), peri-ventricular (PV), or peri-coronary location.

Methods and results Samples of EAT and thoracic subcutaneous fat, obtained from 41 patients paired for cardiovascular risk factors, CAD, and atrial fibrillation were analysed using a pangenomic approach. We found 2728 significantly up-regulated genes in the EAT vs. subcutaneous fat with 400 genes being common between PA, PV, and peri-coronary EAT. These common genes were related to extracellular matrix remodelling, inflammation, infection, and thrombosis pathways. Omentin (*ITLN1*) was the most up-regulated gene and secreted adipokine in EAT (fold-change >12, $P < 0.0001$). Among EAT-enriched genes, we observed different patterns depending on adipose tissue location. A beige expression phenotype was found in EAT but PV EAT highly expressed uncoupled protein 1 ($P = 0.01$). Genes overexpressed in peri-coronary EAT were implicated in proliferation, *O-N* glycan biosynthesis, and sphingolipid metabolism. PA EAT displayed an atypical pattern with genes implicated in cardiac muscle contraction and intracellular calcium signalling pathway.

Conclusion This study opens new perspectives in understanding the physiology of human EAT and its local interaction with neighbouring structures.

Keywords Epicardial adipose tissue • Epicardial fat • Ectopic fat • Microarrays • Beige fat

1. Introduction

Epicardial fat is a metabolically active visceral and perivascular fat depot, surrounding the myocardium and coronary arteries. There is no fascia separating epicardial adipose tissue (EAT) from muscle or vessels, thus allowing a paracrine dialogue between epicardial adipocytes, cardiomyocytes, and cells of the vascular wall.[1,2] The secretion of bioactive inflammatory molecules by the EAT is now recognized as implicated in the formation of atherosclerotic plaques, and the onset of coronary artery disease (CAD).[3–7] The abundance of EAT evaluated by different imaging techniques predicts the number of cardiac events within 8 years, and stent restenosis within 2 years.[8,9] However, a yin-yang

* Corresponding author. Tel: +33 491324504; fax: +33 491254336, E-mail: anne.dutour@ap-hm.fr (A.D.); Tel: +33 1 42 17 79 28/+33 1 44 27 8078, E-mail: karine.clement@psl.aphp.fr (K.C.)
† A.D. and K.C. equally contributed to this work.

role of EAT cannot be excluded. Beyond its secretory capacities, it has been suggested that this depot has beneficial properties such as protecting the coronary arteries against arterial wave torsion, and the heart against hypothermia.[10–12] As such, Sacks *et al.*[13,14] have observed that EAT exhibited features of beige fat, suggesting that this ectopic fat depot could act as a heat-generating tissue around the heart, increasing energy expenditure by producing uncoupling protein 1 . However, the precursors of epicardial adipocytes are still unknown and come out an increasingly investigated research topic. The function of EAT is also not completely understood, particularly at its different locations around the heart. One of the major limitations in studying the physiology of EAT is that only patients with cardiac diseases undergo cardiac surgery. Collecting EAT from healthy subjects would not be possible for obvious ethical reasons. Necropsic studies have shown that EAT does not develop in a homogeneous manner, and that it preferentially accumulates on the free wall of the right ventricle, at the apex of the left ventricle, around atria, epicardial coronary vessels, and appendages.[15–17] Could this preferential localization be an indication of a functional difference? Spiroglou *et al.*[18] reported a different pattern expression of adipokines (adiponectin, visfatin, leptin, chemerin, and vaspin) between pericoronary and apical EAT. The studies carried out on peri-atrial (PA) EAT suggest that the latter are particularly implicated in the incidence of atrial fibrillation, compared with other EAT depots. Nakanishi *et al.*[19] measured the PA fat in 279 patients suspected of having CAD, and showed that the volume of PA fat predicts the risk of *de novo* atrial fibrillation within 3 years, with 88% sensitivity and 92% specificity. *In vitro* studies suggest a local effect of EAT. We have previously shown that human secretory products of EAT, especially adipofibrokines like activin A, induced remodelling of extracellular matrix of rat atrium, ending with myocardial fibrosis.[20] In most studies, the anatomical location of EAT biopsy was not defined or was taken over the right ventricle.

Whether EAT is a global entity, or whether each EAT has a specificity depending on its anatomical location is the question we have addressed in this study by a transcriptomic approach.

2. Objective

The aim of this study exclusively performed in humans was thus to determine a specific EAT signature, depending on its anatomical PA, PV, or peri-coronary location. We thus conducted a pangenomic approach to define a transcriptomic signature of each adipose depot. Our analysis revealed major specific differences in regional EAT's transcriptomic signature involving inflammatory, lipid metabolic, cardiac muscle contraction, and white adipose tissue browning processes.

3. Methods

3.1 Collection of human tissues

The protocol was approved by our local ethics committee of Pitié-Salpêtrière Hospital (Paris) and North Hospital (Marseille). This study was performed in compliance with the Declaration of Helsinki. All patients signed their written informed consent. One hundred and eighteen biopsies ($n = 118$) of paired thoracic subcutaneous and EAT were taken in the same haemodynamic conditions, a few minutes before the extracorporeal circulation was started. Forty-one biopsies were used for microarray, and 77 for explant analysis (see Supplementary material online, *Figure S1*). EAT was collected at one site per patient to minimize the risk of vessel injury and the duration of surgical procedure.

The biopsies of EAT were taken in the PA region (right atrial appendage, $n = 10$), PV area (wall of the right ventricle, $n = 16$), and around pericoronary artery (PCA; at the beginning of the left trunk, between the aorta and the pulmonary artery, $n = 15$; see Supplementary material online, *Figure S2*). The thoracic subcutaneous paired samples were taken from the sternal wall. Patients underwent cardiac surgery for valve replacement or coronary artery bypass grafting, in cardiac surgery departments of two hospitals in Marseille and Paris. The specimens were immediately frozen (-80°C) after collection.

3.2 RNA extraction

RNA was extracted using the Qiagen RNA mini-kit (Dusseldorf, Germany), and total RNA concentration was measured by the use of a Nanodrop 1000 spectrophotometer (Thermo Scientific, DE, USA). RNA quality was verified using the Agilent RNA 600 Nano kit (5067-1511; Agilent, Santa Clara, CA, USA) and read with the 2100 Bioanalyser (Agilent Technologies, Massy, France). Only RNA having an RNA Integrity Number over 4 were amplified.

3.3 Whole-genome gene expression microarrays

Owing to the small sizes of biopsies, 20 ng of the RNA from each sample was amplified, using the kit Ovation Pico SL WTA System V2 (3312-48; Nugen, Bemmel, The Netherlands). Then, the double-stranded purified cDNA were labelled using an Encore BiotinIL Kit (4210-48; Nugen). The labelled cDNA (150 ng) was hybridized onto pangenomic chips, using the HumanHT-12 v4 Expression BeadChip Kit (BD-103-0604; Illumina, San Diego, USA). The chips containing 47 231 probes for 28 688 coded transcripts were read with an iScan Illumina scanner. Hybridization probe intensities were then detected by GenomeStudio. A quantile normalization procedure, without background, was used to eliminate bad quality signals.[21] The difference in gene expression between the thoracic subcutaneous adipose tissue (SAT) and the EAT was performed by the SAM software (significant analysis of microarray, Stanford University, CA, USA; http://www-stat.stanford.edu/~tibs/SAM/index.html), which provides a list of significant genes and an estimate of the false discovery rate (FDR) representing the percentage of genes that could be identified by chance.[22] The FDR was tested at 5 and 10%.

3.4 RT-PCR and PCR

Quantitative RT-PCR was performed with 50 ng of RNA, 200 U of reverse transcriptase SuperScript II (Life Technologies, Saint-Aubin, France), 50 ng of random primers, 10 mM of nucleotides, and 40 U of the ribonuclease inhibitor RNasin (Promega, Charbonnières, France). Primers for quantitative PCR (QuantiTect Primer assays) were designed by Qiagen (Dusseldorf, Germany). Quantitative PCR was performed using primers labelled with fluorescent Sybrgreen (Eurogentec, Angers, France) and a real-time thermocycler, StepOnePlus (Life Technologies). The 18s ribosomal and *GAPDH* RNA were used as reference genes to normalize cycle thresholds (C_t) and to get relative quantification ($\Delta\Delta C_t$), as suggested by others.[23]

3.5 Adipose tissue explants

Explants were made from PV, peri-coronary, and subcutaneous fat from a group of 77 patients who had undergone cardiac valve or coronary artery bypass grafting operations (see Supplementary material online, *Figure S1*), 20 samples were common to microarrays, and 57 new patients were included to confirm the results (see their clinical characteristics in Supplementary material online, *Table S1*), and by incubating 50 mg of the tissue in 500 µL of the culture medium DMEM/HAMF12 (Sigma-Aldrich, St Louis, MO, USA) for 24 h at 37°C, as previously described.[24] After 24 h of incubation, the samples were centrifuged (10 000 *g* for 10 min at 4°C) and the supernatant was removed and stocked at -80°C, prior to analysis.

Quantification of the omentin secreted was done by ELISA using the Human Omentin-1 (EZH0MNTN1-29K; Millipore, Billerica, MA, USA) ELISA kit.

3.6 Western blot

Adipose tissue biopsies were lysed with RIPA (Sigma, Lyon, France), then ground using a Precellys (Ozyme, Montigny-le-Bretonneux, France) tissue homogenizer with CKmix (Ozyme) ceramic beads. The lysates were then centrifuged at 10 000 *g* for 10 min at 4°C. The non-lipid part was removed and placed on a 4–12% Bis-Tris Nupage (Life Technologies) gel, then transferred onto the nitrocellulose membrane (GE Healthcare, Vélizy-Villacoublay, France). The primary antibody against UCP-1 (U6382; Sigma-Aldrich) was used at a dilution of 1/1000. Detection of the primary antibody was made using fluorescent anti-rabbit secondary antibody (926-32211; LI-COR, Courtaboeuf, France) diluted 1/10 000. Signals were read by an Odyssey Scanner (LI-COR).

4. Statistical analysis

Statistical analyses were performed using the software R (R software environment for statistical computing; http://www.R-project.org). Samples of EAT biopsies collected at different locations were matched for patients age, BMI, sex, cardiovascular risk factors, coronary status, and cardiac diseases using ANOVA. We further performed multivariate discriminant analysis to evaluate whether the three groups according to EAT location were comparable. The criteria included were age, CAD status, BMI, diabetes, dyslipidaemia, smoking, hypertension, atrial fibrillation, and sex. The expression profile of each gene was analysed using the programme MeV (Multiple Experiment Viewer), which is a Java application dedicated to microarray analysis. The separation of samples into clusters was done by the Genome Studio Software. The differential expression of each gene was carried out without filtering and correction for multiple testing was systematically performed. The significance level was determined according to the *q*-value of 0.05 or 0.10, which is the adjusted *P*-value for multiple testing using an optimized FDR approach (as defined by the Benjamini–Hochberg method). *q*-value was provided by SAMr package under the R statistical software. The analysis of gene networks was carried out with FunNet[25,26] and presented on Cytoscape, an open source programme networks analysis (Institute of Systems Biology, Seattle, WA, USA). The differences in genes expression quantified by RT-qPCR and the analysis of EAT secretome were performed using the ANOVA and appropriate *post hoc* test. The level of significance used was $P < 0.05$.

5. Results

5.1 Characteristics of the population

Forty-one patients (BMI 28.0 ± 4.5 kg/m^2 and mean age of 67.3 ± 10.4 years) were included in the study. The population studied had a mean LVEF of 57 ± 11%, and 54% had CAD (*Table 1*). Sixty-three per cent patients were treated for hypertension, 54% for dyslipidaemia, 29% were type 2 diabetic subjects, and 49% were smokers. The type and severity of CAD or valvulopathy disease was evenly distributed among groups (see Supplementary material online, *Table S2*). Discriminant multivariate analysis showed that the three groups according to EAT location were not different according to age, CAD status, BMI, diabetes, dyslipidaemia, smoking, hypertension, atrial fibrillation, and sex, and that the matching was sufficient to draw analysis (*Figure 1*).

5.2 Specific pattern of EAT reveals a brite/beige phenotype

The mean number of detected genes was 9700 ± 105. Analysis of the hierarchical cluster tree on MeV showed that EAT depots clustered differently from SAT, and that among EAT, PA EAT clustered apart (see Supplementary material online, *Figure S3*).

The SAM procedure identified 2123 genes (at FDR = 5) and 2728 (at FDR = 10) significantly overexpressed in the EAT (all depots together), compared with subcutaneous thoracic adipose tissue, whereas 2227 (FDR = 10) genes were significantly down-regulated in EAT, compared with SAT (*Table 2*). See Supplementary material online, *Figure S4* illustrates the biological themes characterizing the transcriptomic signature of total EAT. The functional analysis of genes,

Table 1 Characteristics of the four adipose tissue groups (peri-atrial, peri-right ventricular, peri-coronary, and thoracic subcutaneous) in the population studied

	peri-atrial	Peri-right ventricle	Peri-coronary artery	thoracic subcutaneous	*P*-value
N	10	16	15	41	
Sex ratio, *n* (%)	7 (70)	12 (75)	11 (73)	24 (77)	0.98
Age (years)	70.3 ± 11.2	65.4 ± 12.2	67.4 ± 7.5	66.4 ± 10.1	0.71
Coronary status, *n* (%)	6 (60)	9 (56)	6 (40)	16 (52)	0.93
Valvulopathy	4 (40)	7 (44)	8 (53)	15 (48)	0.93
BMI (kg/m^2)	28.7 ± 4.5	27.9 ± 4.6	27.6 ± 4.7	27.8 ± 4.5	0.82
BMI range	21–35	18–37	22–37	18–37	
Type 2 diabetes, *n* (%)	2 (20)	5 (31)	5 (33)	10 (32)	0.93
Atrial fibrillation, *n* (%)	2 (20)	3 (19)	6 (40)	9 (29)	0.58
LVEF (%)	58 ± 13	53 ± 11	61 ± 8	57 ± 10	0.29
Heart failure (LVEF < 50%), *n* (%)	1 (10)	2 (12)	1 (7)	3 (10)	1
Hypertension, *n* (%)	7 (70)	10 (62)	9 (60)	19 (61)	0.97
Dyslipidaemia, *n* (%)	5 (50)	9 (56)	8 (53)	17 (55)	1
Smoking status, *n* (%)	6 (60)	9 (56)	5 (33)	14 (45)	0.51

annotated with categories of the Kyoto Encyclopedia of Genes and Genomes (KEGG), revealed that total EAT was mainly related to cell–cell interaction, oxidative phosphorylation, and cardiac muscle contraction pathways. Peroxisome proliferator-activated receptor (PPAR) gamma signalling and fatty acid metabolism themes were down-regulated in EAT compared with SAT (see Supplementary material online, *Figure S4*). Gene ontology analyses also revealed a specific signature of EAT in muscular differentiation, suggesting a possible 'beige' or 'brite' phenotype. Indeed, EAT expressed certain specific genes of the brown adipose tissue such as *ACTA1*, actin alpha 1 (*ACTC1*), PPAR gamma co-activator 1 alpha (*PPARGC1A*), troponin C type 1, and troponin I type 1. In addition, the homeobox C9 (*HOXC9*) gene was significantly down-regulated in EAT compared with SAT, translating into an intermediary 'beige' or 'brite' profile of EAT (*Figure 2*). While we were not able to detect *UCP-1* gene in our microarray setting (FDR >10), *UCP-1* gene expression evaluated by qPCR was significantly up-regulated in EAT In agreement, UCP-1 protein was significantly increased in EAT, using western blotting (*Figure 2*).

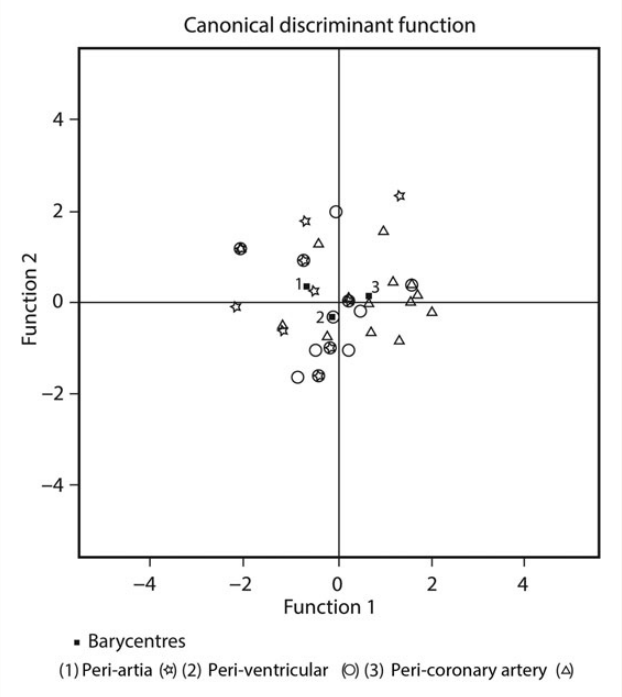

Figure 1 Discriminant multivariate analysis showing the distribution of patients among EAT location groups according to clinical parameters. The clinical criteria included were age, CAD status, BMI, diabetes, dyslipidaemia, smoking, hypertension, atrial fibrillation, and sex. One symbol can represent several patients. Squares represent the barycentres of groups (1, peri-atrial; 2, peri-ventricular and 3, peri-coronary artery).

5.3 Common EAT characteristics

We further focused on EAT-enriched genes. Venn diagram analysis identified that the three groups of EAT shared 400 common genes (*Figure 3A*; see Supplementary material online, *Table S3*). Gene ontology analysis revealed that these 400 genes are involved in biological processes including (i) extracellular matrix remodelling, associated with collagen IV, VI, thrombospondin 3, laminin alpha 2, fibronectin 1 genes; (ii) thrombosis, together with tissue plasminogen activator, prostaglandin D2 synthase (*PTGDS*), and inflammatory/infectious *sPLA2-IIA* (Group IIA secretory phospholipase A2) genes, as shown previously[24]; and (iii) inflammation/infection, associated with genes encoding complement factors (*Figure 3B*). Among these shared genes, *ITLN1* (omentin), synaptotagmin IV (SYT4), complement factor B (*CFB*), ezrin (*EZR*), indolethylamine *N*-methyltransferase (*INMT*), proteoglycan 4 (PRG4), and arachidonate 15-lipoxygenase (*ALOX15*) genes were highly up-regulated compared with SAT (2.27–13.73-fold-change, *q*-value = 0.00). These results were confirmed using RT-qPCR and showed that these seven genes were the most abundantly expressed genes in EAT (*Figure 4*). Omentin (*ITLN1*) was the most up-regulated gene in EAT (fold-change >12). Gene network analysis with cytoscape showed that omentin was closely co-expressed with 79 other genes (see Supplementary material online, *Table S4*), suggesting an important connecting role for this adipokine (*Figure 5*).

5.4 Specific signatures characterize different EAT depots

Beige signature was particularly pronounced in the PV EAT, as *UCP-1* expression was five-fold higher in PV EAT compared with PA EAT ($P = 0.01$), $P = 0.08$ compared with the peri-coronary EAT by trend (*Figure 2*). Omentin expression was significantly higher in PV EAT, compared with other EAT depots. Omentin secretion was also highly increased in the PV EAT compared with the subcutaneous and the peri-coronary EAT (both, $P < 0.0001$), in agreement with qPCR results. However, due to the tiny size (<20 mg of tissue) of the biopsies obtained from the PA EAT, omentin secretion measurements were not available in this tissue (*Figure 5*).

Remarkably, we observed a specific expression signature for PA, PV, and peri-coronary EAT. We precisely identified 2571 genes enriched in PA EAT, 622 genes enriched in PV EAT, and 1170 in peri-coronary (PCA)

Table 2 Paired analyses of the number of genes differently expressed between each EAT and SAT at FDR = 5 and 10

	PCA vs. SAT		PV vs. SAT		PA vs. SAT		Total EAT vs. SAT	
	FDR 5	FDR 10	FDR 5	FDR 10	FDR 5	FDR 10	FDR 5	FDR 10
No. of genes up-regulated	1731	2540	1122	1587	2767	3682	2123	2728
No. of genes down-regulated	1446	1945	827	1105	2546	3309	1813	2227
Total	3177	4485	1949	2692	5313	6991	3936	4955

No., number; PCA, peri-coronary artery; PV, peri-right ventricle; PA, peri-atrial.

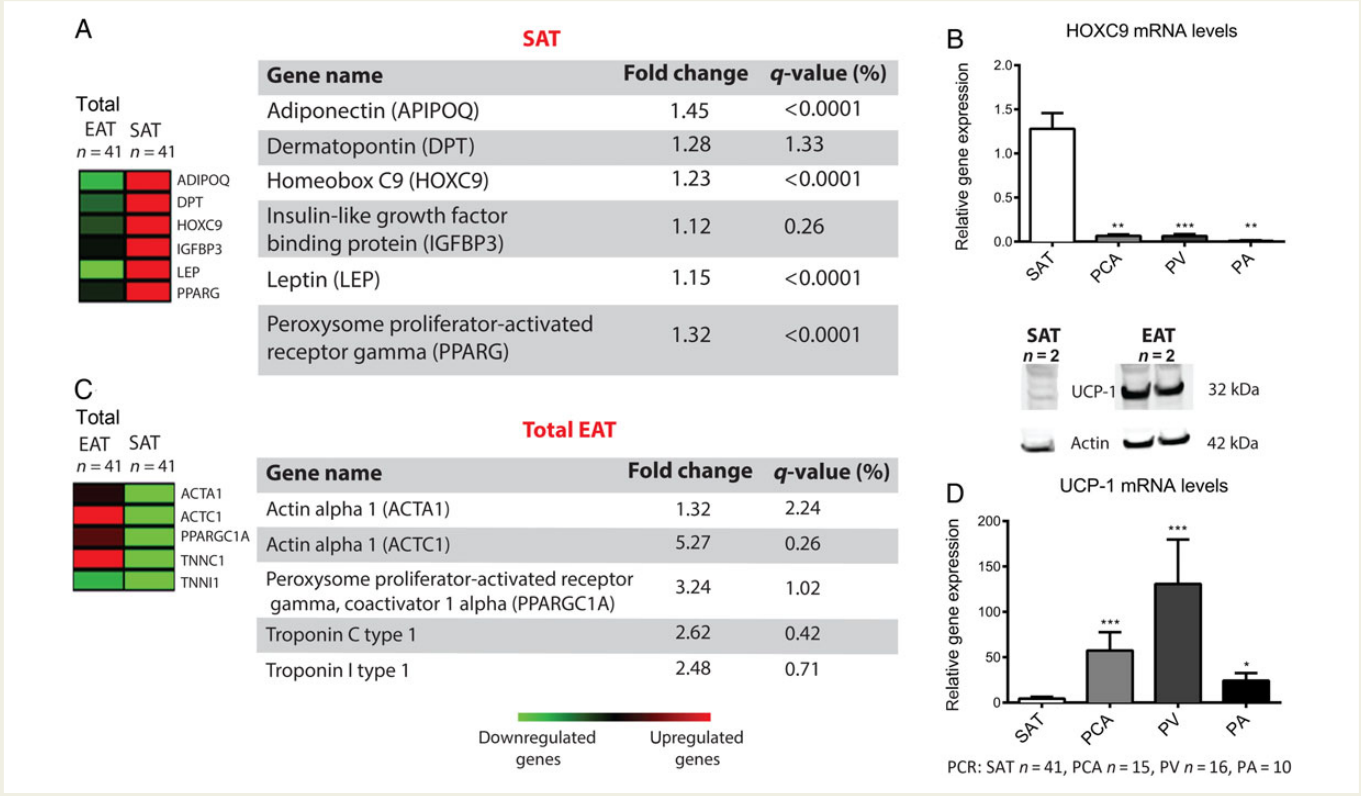

Figure 2 Characteristics of EAT 'beige'/'brite' profile. (*A*) Heat map of white adipose tissue-enriched genes. (*B*) Expression of *HOXC9* in each EAT (qPCR) (PA, PV, and PCA, compared with SAT. (*C*) Heat map of genes characterizing 'browning' in white adipose tissue. (*D*) Gene expression and protein content of *UCP-1* in EAT compared with SAT. *$P < 0.05$ vs. SAT; **$P < 0.01$ vs. SAT; ***$P < 0.0001$ vs. SAT. *q*-values in *A* and *C* are the smallest FDR at which each particular gene would just stay on the list of positive genes.

EAT. PA EAT was identified as the most atypical EAT, with regard to pangenomic profile (see Supplementary material online, *Figure S3*).

Network analyses of these genes using FunNet showed that the PV EAT overexpressed genes remarkably implicated in Notch/p53 (*CHK1*, *DAAM1*, *IGF1*, and *SHISA5*), inflammation (*TNF-R1*, *STAT1*, and *SERPING1*), ABC transporters (*ABCA8* and *ABCD4*), or glutathione metabolism (*GSTO2*, *GSR*, and *GSTP1*). The peri-coronary EAT overexpressed genes implicated in proliferation (*CycB*, *CycE1*, *CycD*, and *CDK6*), *O-N* glycan biosynthesis (*GTB*, *CD68*, *POFUT2*, and *ALG6*), and sphingolipid metabolism (*GLB1*, *SGPP2*, and *SIAL3*). The PA EAT overexpressed genes implicated in oxidative phosphorylation (*COXs* and *ATPs*), cell adhesion (*ANKRD1*, *TNC*, and *COL4A4*), cardiac muscle contraction (*TNNI3*, *TPMs*, *ACTC1*, and *MYH6*), and intracellular calcium signalling pathway (*SERCA1*, *CAMK2B*, *CAMK2D*, and *NCX2*), suggesting a specific contribution of PA EAT to cardiac muscle activity (*Figure 6*).

The differences shown in the three EAT gene expression were not linked to patients' characteristics, as the expression of adiponectin, leptin, *HOXC9*, *PGC1α*, *EZR*, *INMT* using PCR, and microarrays were similar in their subcuteanous adipose tissue counterpart (*Figures 7* and *8*).

6. Discussion

Using gene-profiling analysis, we here described that the EAT presents different characteristics from the thoracic SAT, and especially shows an overexpression of gene characteristics of a 'beige'/'brite' phenotype. The novelty of our work is to propose a new transcriptomic characterization of EAT, depending on its anatomical cardiac localization.

6.1 Common EAT gene profile

First, the three EAT depots share highlighting of inflammation, extracellular matrix remodelling, and thrombosis pathways. This strengthens previous observations describing the differences between abdominal visceral and SAT located in the periumbilical area in obese patients.[27–29] It has also been reported that EAT is more inflamed than SAT, particularly in CAD patients; it secretes pro-inflammatory cytokines such as TNF-α, IL-6, MCP-1, IL-1β, and NLRP3, and is infiltrated by immune cells, especially by macrophages with an M1 profile.[6,7,30] Few studies compared the transcriptomic profiles of EAT with those of visceral adipose tissue, since both abdominal and thoracic cavities need to be opened simultaneously to reach tissues. Only, Imoto-Tsubakimoto *et al.*[31] have shown the up-regulation of 55 genes implicated in the inflammatory immune response in EAT vs. visceral abdominal adipose tissue. Among these 55 genes, 35 genes, including *IL-1β*, *IL-6*, *IL-8*, and the chemokine receptor 2 genes, were expressed twice as much in the EAT than in the visceral adipose tissue, suggesting that the EAT, although it represents <1% of the global adipose tissue mass, is more inflamed than the visceral abdominal depot.

Taken together with the induction of pro-inflammatory factors, we confirmed observations showing that EAT is characterized by a signature of extracellular matrix and remodelling genes including collagen types, profibrotic factors, and remodelling enzymes. The induction of the

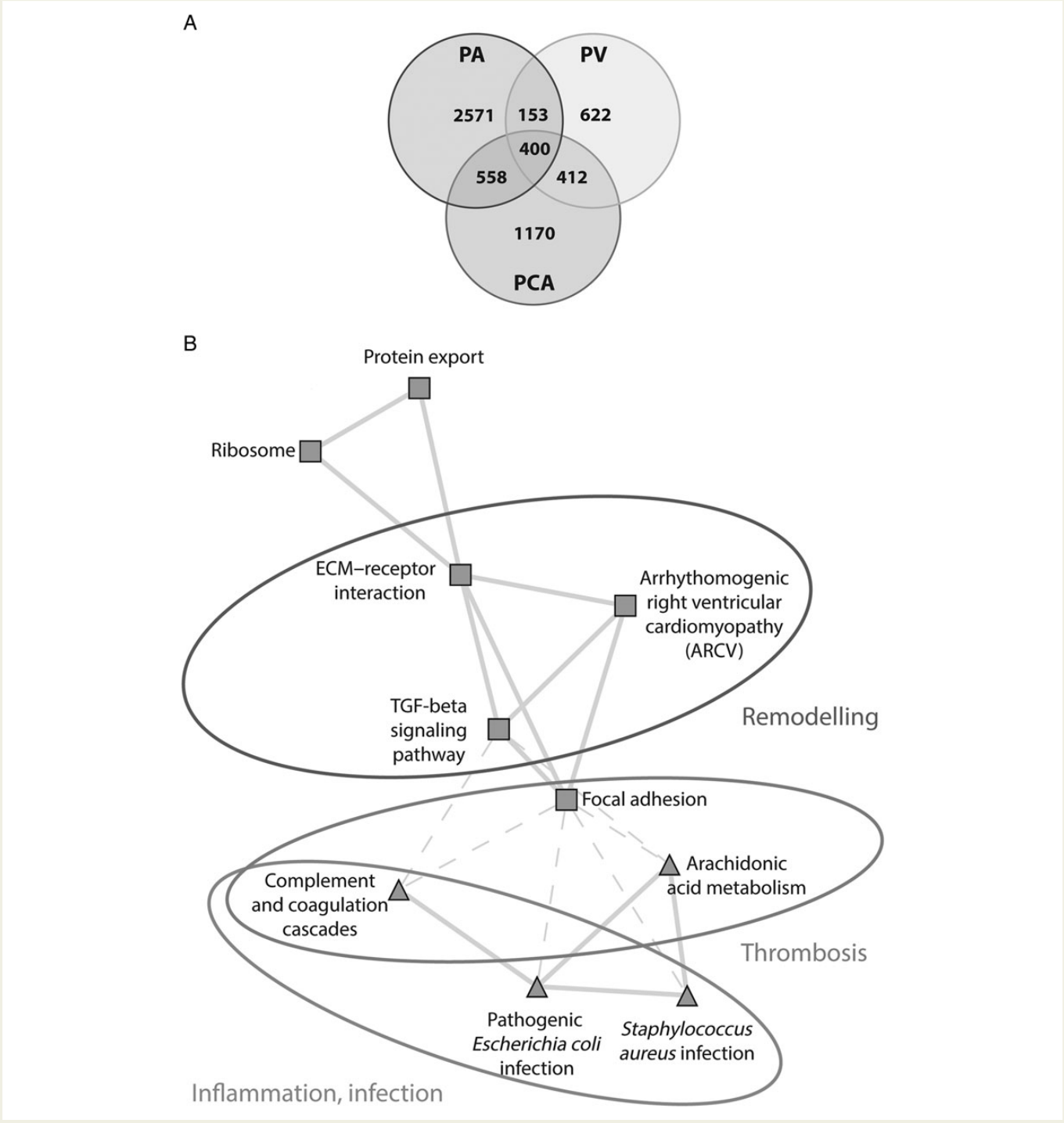

Figure 3 (*A*) Venn diagram. (*B*) Functional analysis of common genes shared by the three epicardial tissues (PA, PV, and PCA; KEGG and cytoscape analyses) at FDR = 10.

extracellular matrix remodelling genes in the visceral adipose tissue of mice kept on a high fat diet has already been described.[32] Similar findings were reported in the subcutaneous and omental adipose tissue of obese subjects.[27,33] At variance of other adipose depots, the abundance of epicardial fat fibrosis has never been properly quantified. Nevertheless, this expression and secretion of profibrotic factors may have functional consequences on the adjacent myocardium and atrium.

As such, we have previously shown that the secretory products of EAT can induce myocardial fibrosis of rat atria.[20] In addition, our group has previously described the induction of genes implicated in thrombosis, especially *sPLA2-IIA* (Group IIA secretory phospholipase A2) in EAT, a phospholipase present in atherosclerotic lesions, which has a crucial role in the pro-inflammatory cascade.[24] Overexpression of *PTGDS* in EAT has also been already observed elsewhere.[34] The similarities observed in other studies further substantiate our data and strengthen the hypothesis that EAT is implicated in inflammatory, immune, and remodelling processes, independently of CAD status.

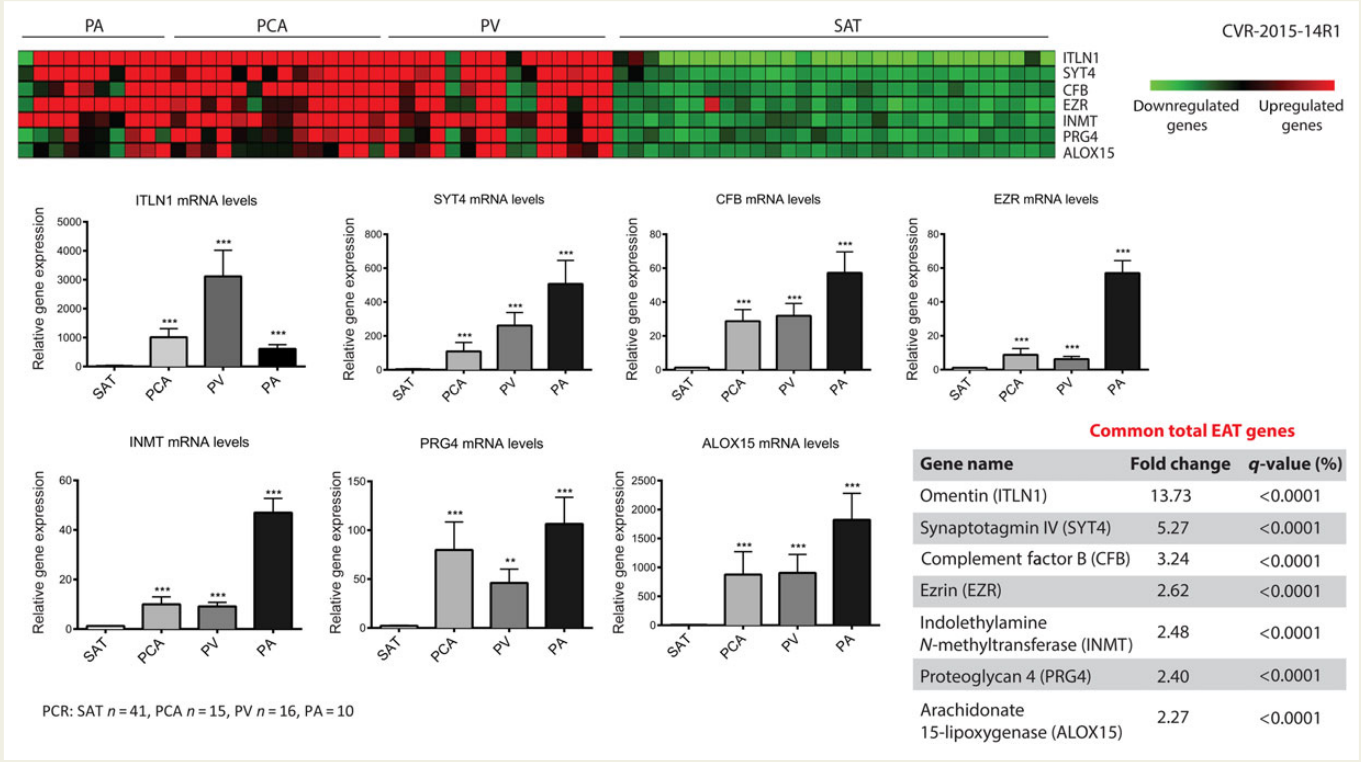

Common total EAT genes

Gene name	Fold change	*q*-value (%)
Omentin (ITLN1)	13.73	<0.0001
Synaptotagmin IV (SYT4)	5.27	<0.0001
Complement factor B (CFB)	3.24	<0.0001
Ezrin (EZR)	2.62	<0.0001
Indolethylamine *N*-methyltransferase (INMT)	2.48	<0.0001
Proteoglycan 4 (PRG4)	2.40	<0.0001
Arachidonate 15-lipoxygenase (ALOX15)	2.27	<0.0001

Figure 4 The top seven common up-regulated genes in EAT compared with SAT (fold-change >2), and their validation by quantitative PCR. $^{**}P < 0.01$ vs. SAT; $^{***}P < 0.0001$ vs. SAT.

6.2 Beige phenotype

Secondly, we have shown that EAT could have a 'beige' profile, due to the overexpression of *UCP-1*, and to several genes characterizing adipose tissue 'browning'. The 'brite' (i.e. brown in white) or 'beige' adipocytes are multi-locular adipocytes located within white adipose tissue islets, which have the capacity to be recruited and to express *UCP-1*, mainly in case of cold exposure. Beige adipocytes do not come from the dermomyotomal precursor shared by brown adipose tissue and muscle.[35–37] These adipocytes have a specific molecular signature, which is currently being identified, and coexist with brown adipose tissue.[38–40] Sacks *et al.*[13,14] have reported beige molecular signature of EAT taken from the start of the right coronary artery. Our results corroborate those of Sacks *et al.*, and show in addition that the PV EAT could be the more sensitive to 'browning'. This has to be confirmed in functional studies. Genes enriched in PV EAT encode enzymes of the glutathione metabolism pathway. The enzymes, implicated in the metabolism of glutathione, have a specific signature in brown adipose tissue, due to the decoupling of the respiratory chain, the increase in oxidative metabolism, and H_2O_2 production.[41] It has been proposed that beige adipose tissue in EAT originates from the recruitment of white adipocytes whose browning is induced by factors such as myokines or growth factors like irisin, FGF21, or cardiac natriuretic peptides (atrial natriuretic peptide/brain natriuretic peptide).[40,42] Whether these factors have a direct paracrine effect on EAT remains to be determined.

6.3 Omentin

We have observed that one of the most expressed genes in EAT was omentin (*ITLN-1*). This adipokine is secreted markedly by EAT as opposed to the SAT. It has already been reported that omentin has beneficial anti-inflammatory properties, and that it promotes insulin sensitivity.[43,44] Studies have shown that omentin ameliorates endothelial function, and reperfusion after ischaemia, by increasing the production of nitric oxide by endothelial NO synthase.[45–47] Its plasma level decreases in obesity and in type 2 diabetes.[48,49] Fain *et al.*[50] have shown that it was secreted by the stromal vascular fraction of EAT. Greulich *et al.*[51] showed that contractile dysfunction of cardiomyocytes exposed to EAT conditioned media of diabetic patients was improved by the addition of recombinant omentin *in vitro*. As a whole, this gene expression study confirms the fact that EAT produces factors having both positive and deleterious effect on the heart.

6.4. Specific transcriptomic signature of EAT

Our observations are substantiated by the identification of a transcriptomic signature associating with perivascular (peri-coronary), PA, or PV anatomical location. While most studies use samples taken from regions close to the root of the right coronary artery,[6,13] we identify for the first time signatures of gene enrichments for each of the peri-coronary, PV, and PA EAT. At variance of our expectation, we observed that peri-coronary EAT is not the more pro-inflammatory depot at least at the gene expression level. PV EAT appears more closely linked to the genes involved in inflammation and immunity processes. PV EAT is also characterized by genes of the A, B, and C transporters, which are implicated in cellular detoxification and intracellular lipid transport.[52,53] The peri-coronary EAT associates with cyclin and cell cycle pathway genes, but also with the sphingolipid metabolism pathway. Sphingolipids are complex lipids present in atherosclerotic plaques. They induce

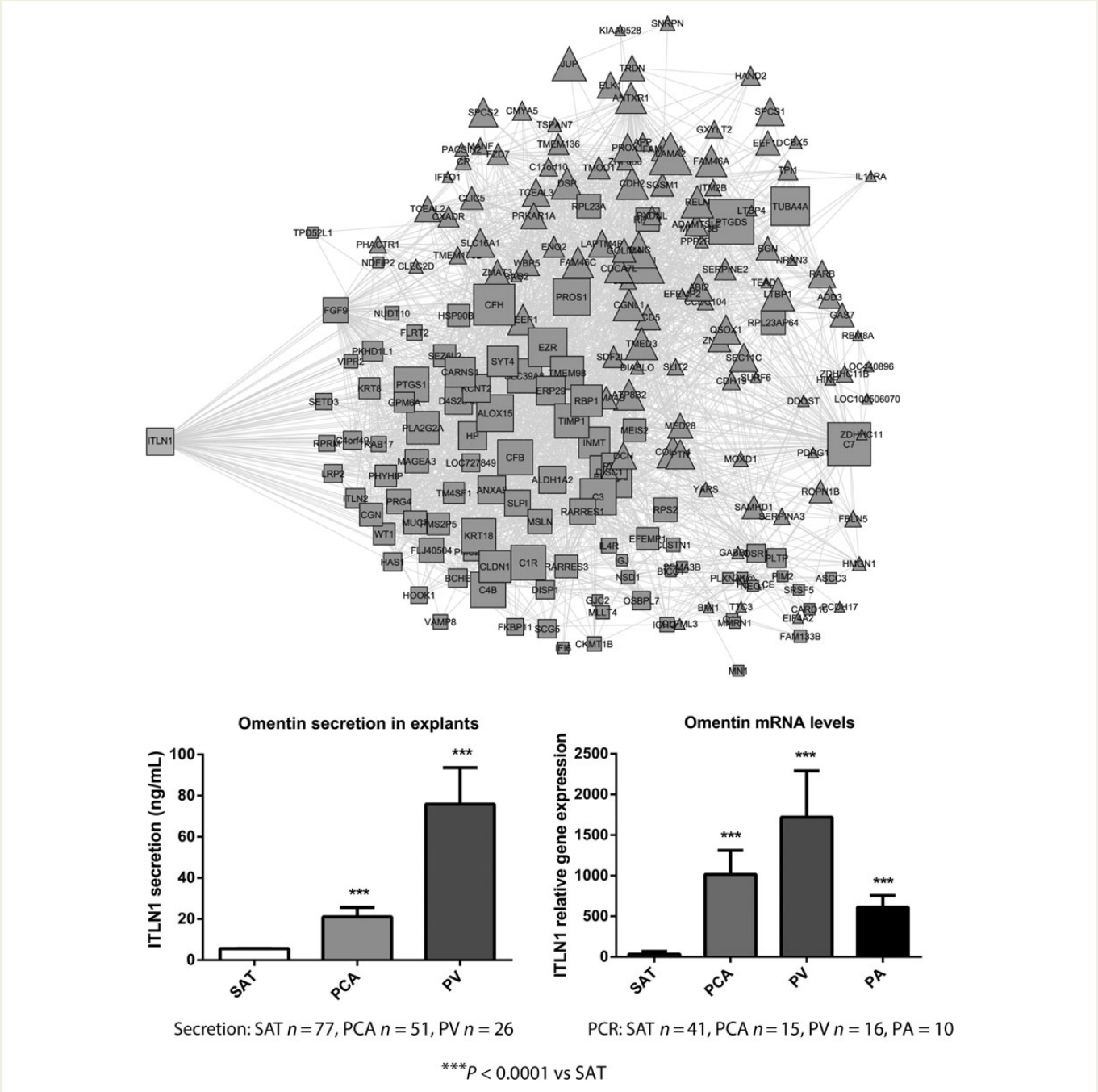

Figure 5 Expression and secretion of omentin (ITLN1) in each EAT (PA, PV, and PCA) compared with SAT. *ITLN1* gene interconnections with other up-regulated genes. ***$P < 0.0001$ vs. SAT.

aggregation and retention of oxidized LDL and VLDL in the sub-endothelial space, which in turn increases the capture of aggregated lipoproteins by macrophages and their transformation into foam cells.[54,55] Owing to its perivascular location, the peri-coronary EAT seems to be more implicated in atherogenesis. It can also be hypothesized that the activation of the sphingolipid pathway is a sign of toxic lipid derivatives accumulation in the vascular wall. One could also suggest that the peri-coronary EAT is implicated in the transfer of 'outside in' lipids, from the EAT towards systemic circulation.

Finally, we observed that the PA EAT is an atypical adipose tissue, different from the other two EATs, by expressing genes implicated in oxidative phosphorylation, muscular contraction, and calcium signalling. This is in accordance with the study of Nakanishi *et al.*[19] that has found an association between PA EAT and new-onset non-valvular atrial fibrillation. The *SERCA1* gene, which is significantly overexpressed in the PA EAT, codes for a Ca^{2+}/ATP-dependent intracellular pump that translocates the cytosolic calcium into the lumen of the sarcoplasmic reticulum, and promotes excitation–contraction coupling.[56,57] Furthermore, induction of genes, such as heavy chains of myosin and tropomyosins, is in favour of a strong interaction between PA EAT and cardiac muscle.[58] However, the presence of genes coding for proteins implicated in cardiomyocyte contraction questions the type of

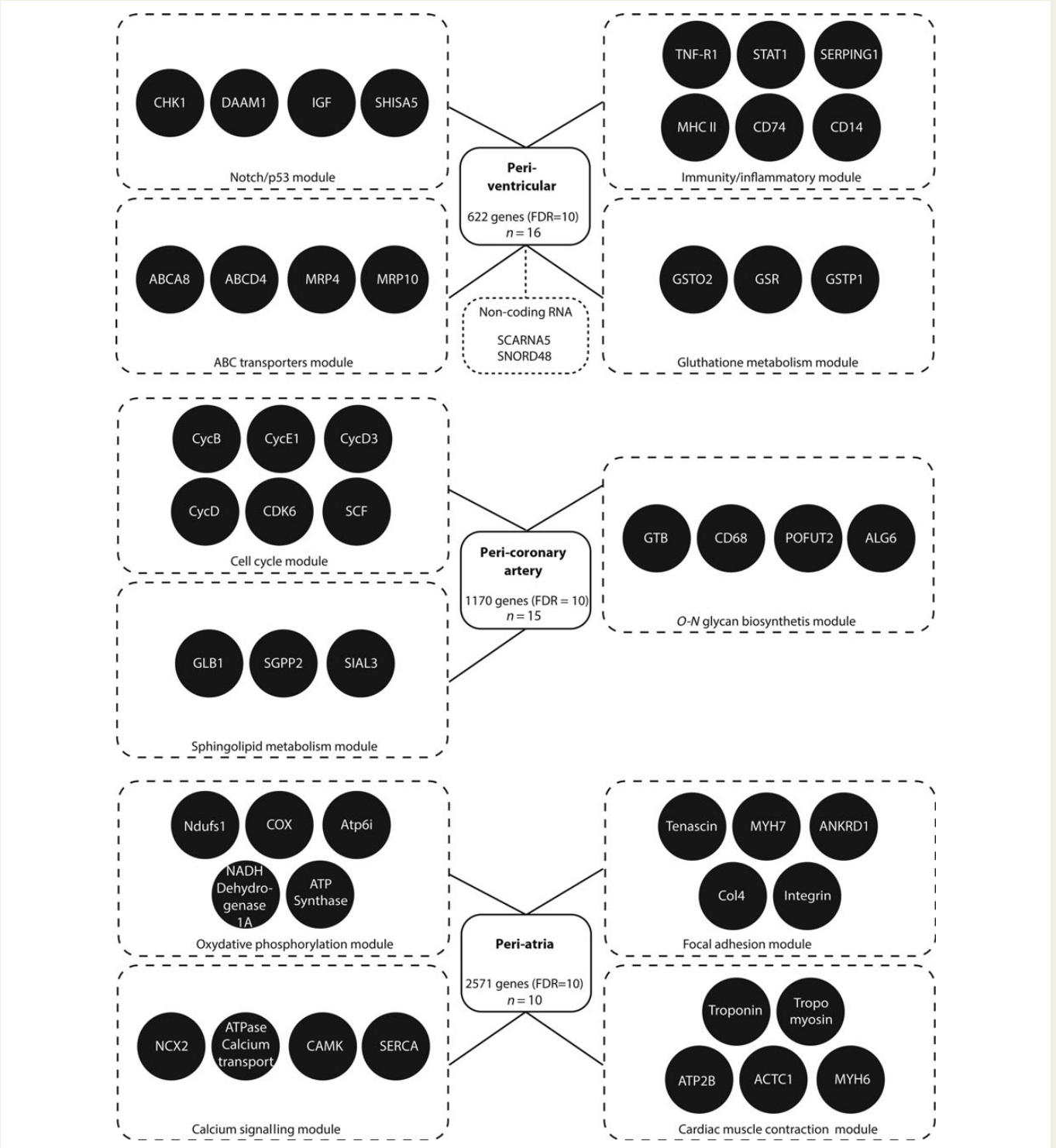

Figure 6 Identification of an enrichment signature for peri-atrial, peri-ventricular, and peri-coronary artery EAT, according to cytoscape genes network analysis. The top of the up-regulated genes is shown in circles (at FDR = 10).

subcellular compartment expressing these genes. Cellular types composing adipose tissue include mature adipocytes and a variety of other cells grouped in the stroma vascular fraction such as immune cells and progenitors. Nevertheless, given the small quantity of EAT in the peri-atrium, and the tiny biopsy sizes (<20 mg), infiltration of the PA tissue biopsies by muscle cells cannot be excluded.

6.5 Limitations

This study has several limitations: the analysis of samples from healthy subjects would have been more interesting to study the EAT physiology. However, this was not possible for obvious ethical reasons, and cardiac surgery is the only way to get EAT biopsies, implying to adjust the samples for cardiovascular risk factors, CAD, and atrial

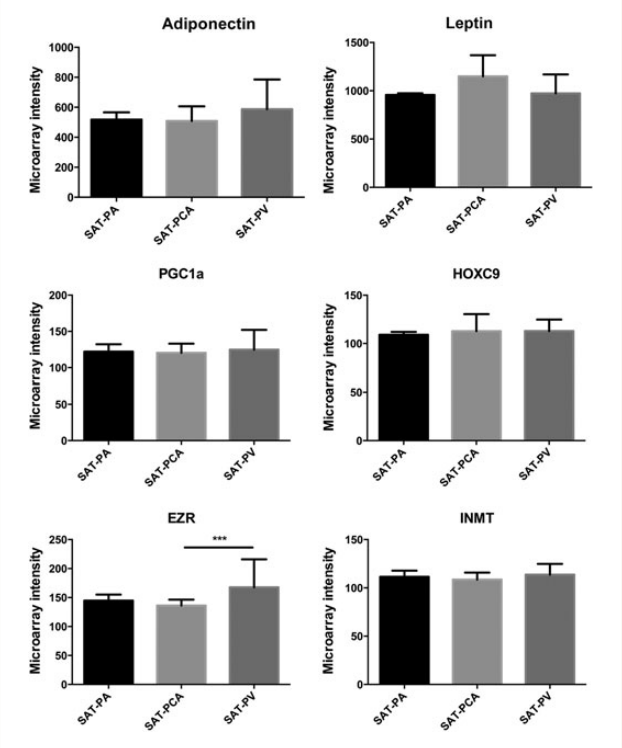

Figure 7 Comparison of several gene expression in the SAT of patients with PA, PV, and PCA EAT biopsies, using microarrays. *P* = non-significant. *HOXC9*, homeobox C9; *PGC1α*, peroxisome proliferative activated receptor, gamma, coactivator 1 alpha; *EZR*, ezrin; *INMT*, indolethylamine *N*-methyltransferase.

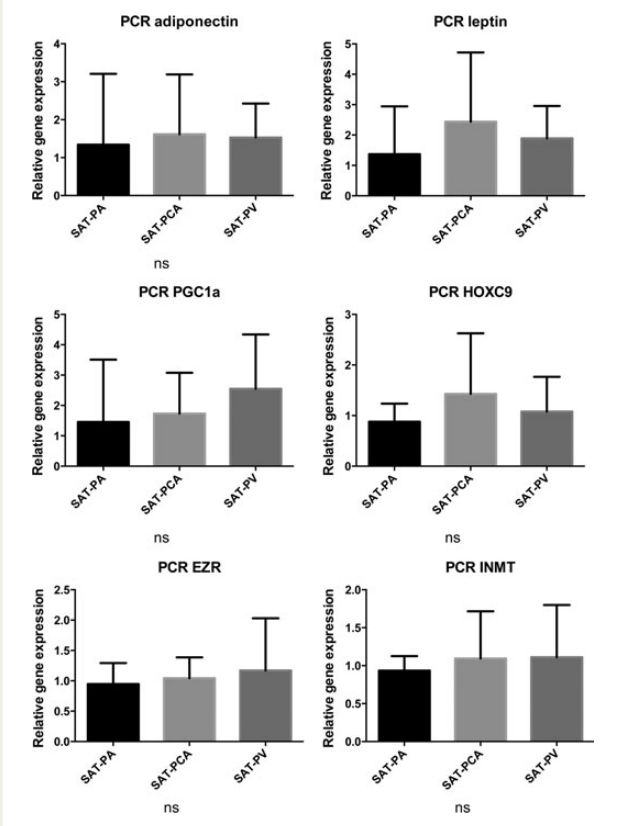

Figure 8 Comparison of several gene expression in the SAT of patients with PA, PV, and PCA EAT biopsies, using quantitative PCR (*n* = 41); *P* = non-significant. *HOXC9*, homeobox C9; *PGC1α*, peroxisome proliferative activated receptor, gamma, coactivator 1 alpha; *EZR*, ezrin; *INMT*, indolethylamine *N*-methyltransferase.

fibrillation status. Paired biopsies of the four locations from the same patients would have been more accurate to draw analyses and conclusions, but would have significantly increased the time and risk of the procedure. However, similar gene expression was found in the subcutaneous fat of the three groups of patients with EAT biopsies, suggesting that the differences shown in our work were not due to differences in patients characteristics but to differences in tissue characteristics. Furthermore, discriminant multivariate analysis showed that we could not discriminate the three groups of EAT according to clinical parameters. As such, specific transcriptomic signature depending on anatomical location of EAT is likely, but needs to be explored further in both clinical and experimental settings.

In this study, we provided one comprehensive list of transcriptomic signatures that characterize EAT depots associated with anatomical locations. This could suggest different functions with respect to the structures adjacent to it, and reveals the importance of taking into account the origin of EAT biopsies or explants in further *in vitro* studies. For *in vivo* future clinical research, our study reveals that it is important not to consider EAT as a whole entity but to focus on each compartment. Imaging assessment of each EAT compartment might add a value in the risk of CAD, and decrease the time of post-processing computed tomography or magnetic resonance imaging measurements. Furthermore, our study provides another illustration that EAT expresses and secretes molecules, which could have a deleterious but also a cardioprotective effect as shown for omentin. Thus, limiting the role of EAT to a harmful effect on the vascular wall and on cardiac function would be very reductive. The implication of EAT in the pathophysiology of CAD is probably the result of an imbalance between pro-inflammatory, proatherogenic bioactive molecules, and cardioprotective insulin-sensitizing molecules such as omentin.[59] Our study provides additional information regarding the central place occupied by ectopic fat on local organ metabolism and function, and will bring new insights in adipocyte–myocyte cross-talk and pathophysiology.

Supplementary material

Supplementary material is available at *Cardiovascular Research* online.

Acknowledgements

We thank Wassila Carpentier for her skilled technical assistance in microarrays (P3S-platform at Pitié-Salpêtrière hospital). We are grateful for the patients and their surgeons, and Dr Patrick Farahmand who provided access to human tissues in accordance with ethics laws. We also thank Edi Prifti and Aurélie Cotillard for their statistical help. We thank Florent Louault for help in collecting samples. We thank Froogh Hajduch for checking English language.

Conflict of interest: none declared.

Funding

This work was supported by the French National Agency through the national program 'Investissements d'avenir' with the reference (ANR-10-IAHU-05)

and the ANR program 'Adipofib'. B.G. and K.C. were supported by a grant from FRM (Fondation Pour la Recherche Médicale, FRM (DEQ20120323701). S.N.H. was supported by a grant from European Network for Translational Research in atrial fibrillation (FP7 collaborative project EUTRAF, grant no. 261057).

References

1. Guzzardi MA, Iozzo P. Fatty heart, cardiac damage, and inflammation. *Rev Diabet Stud* 2011;**8**:403–417.
2. Cherian S, Lopaschuk GD, Carvalho E. Cellular cross-talk between epicardial adipose tissue and myocardium in relation to the pathogenesis of cardiovascular disease. *Am J Physiol Endocrinol Metab* 2012;**303**:E937–E949.
3. Gaborit B, Kober F, Jacquier A, Moro PJ, Flavian A, Quilici J, Cuisset T, Simeoni U, Cozzone P, Alessi MC, Clement K, Bernard M, Dutour A. Epicardial fat volume is associated with coronary microvascular response in healthy subjects: a pilot study. *Obesity (Silver Spring)* 2012;**20**:1200–1205.
4. Iacobellis G, Gao YJ, Sharma AM. Do cardiac and perivascular adipose tissue play a role in atherosclerosis? *Curr Diab Rep* 2008;**8**:20–24.
5. Karastergiou K, Evans I, Ogston N, Miheisi N, Nair D, Kaski JC, Jahangiri M, Mohamed-Ali V. Epicardial adipokines in obesity and coronary artery disease induce atherogenic changes in monocytes and endothelial cells. *Arterioscler Thromb Vasc Biol* 2010;**30**:1340–1346.
6. Mazurek T, Zhang L, Zalewski A, Mannion JD, Diehl JT, Arafat H, Sarov-Blat L, O'Brien S, Keiper EA, Johnson AG, Martin J, Goldstein BJ, Shi Y. Human epicardial adipose tissue is a source of inflammatory mediators. *Circulation* 2003;**108**:2460–2466.
7. Shimabukuro M, Hirata Y, Tabata M, Dagvasumberel M, Sato H, Kurobe H, Fukuda D, Soeki T, Kitagawa T, Takanashi S, Sata M. Epicardial adipose tissue volume and adipocytokine imbalance are strongly linked to human coronary atherosclerosis. *Arterioscler Thromb Vasc Biol* 2013;**33**:1077–1084.
8. Mahabadi AA, Berg MH, Lehmann N, Kalsch H, Bauer M, Kara K, Dragano N, Moebus S, Jockel KH, Erbel R, Mohlenkamp S. Association of epicardial fat with cardiovascular risk factors and incident myocardial infarction in the general population: the Heinz Nixdorf Recall Study. *J Am Coll Cardiol* 2013;**61**:1388–1395.
9. Park JS, Choi BJ, Choi SY, Yoon MH, Hwang GS, Tahk SJ, Shin JH. Echocardiographically measured epicardial fat predicts restenosis after coronary stenting. *Scand Cardiovasc J* 2013;**47**:297–302.
10. Iacobellis G, Corradi D, Sharma AM. Epicardial adipose tissue: anatomic, biomolecular and clinical relationships with the heart. *Nat Clin Pract Cardiovasc Med* 2005;**2**:536–543.
11. Rabkin SW. Epicardial fat: properties, function and relationship to obesity. *Obes Rev* 2007;**8**:253–261.
12. Sacks HS, Fain JN. Human epicardial adipose tissue: a review. *Am Heart J* 2007;**153**:907–917.
13. Sacks HS, Fain JN, Bahouth SW, Ojha S, Frontini A, Budge H, Cinti S, Symonds ME. Adult epicardial fat exhibits beige features. *J Clin Endocrinol Metab* 2013;**98**:E1448–E1455.
14. Sacks HS, Fain JN, Holman B, Cheema P, Chary A, Parks F, Karas J, Optican R, Bahouth SW, Garrett E, Wolf RY, Carter RA, Robbins T, Wolford D, Samaha J. Uncoupling protein-1 and related messenger ribonucleic acids in human epicardial and other adipose tissues: epicardial fat functioning as brown fat. *J Clin Endocrinol Metab* 2009;**94**:3611–3615.
15. Corradi D, Maestri R, Callegari S, Pastori P, Goldoni M, Luong TV, Bordi C. The ventricular epicardial fat is related to the myocardial mass in normal, ischemic and hypertrophic hearts. *Cardiovasc Pathol* 2004;**13**:313–316.
16. Schejbal V. [Epicardial fatty tissue of the right ventricle—morphology, morphometry and functional significance]. *Pneumologie* 1989;**43**:490–499.
17. Tansey DK, Aly Z, Sheppard MN. Fat in the right ventricle of the normal heart. *Histopathology* 2005;**46**:98–104.
18. Spiroglou SG, Kostopoulos CG, Varakis JN, Papadaki HH. Adipokines in periaortic and epicardial adipose tissue: differential expression and relation to atherosclerosis. *J Atheroscler Thromb* 2010;**17**:115–130.
19. Nakanishi K, Fukuda S, Tanaka A, Otsuka K, Sakamoto M, Taguchi H, Yoshikawa J, Shimada K, Yoshiyama M. Peri-atrial epicardial adipose tissue is associated with new-onset nonvalvular atrial fibrillation. *Circ J* 2012;**76**:2748–2754.
20. Venteclef N, Guglielmi V, Balse E, Gaborit B, Cotillard A, Atassi F, Amour J, Leprince P, Dutour A, Clement K, Hatem SN. Human epicardial adipose tissue induces fibrosis of the atrial myocardium through the secretion of adipo-fibrokines. *Eur Heart J* 2015;**36**:795–805a.
21. Smyth GK, Speed T. Normalization of cDNA microarray data. *Methods* 2003;**31**:265–273.
22. Tusher VG, Tibshirani R, Chu G. Significance analysis of microarrays applied to the ionizing radiation response. *Proc Natl Acad Sci USA* 2001;**98**:5116–5121.
23. Chechi K, Gelinas Y, Mathieu P, Deshaies Y, Richard D. Validation of reference genes for the relative quantification of gene expression in human epicardial adipose tissue. *PLoS ONE* 2012;**7**:e32265.
24. Dutour A, Achard V, Sell H, Naour N, Collart F, Gaborit B, Silaghi A, Eckel J, Alessi MC, Henegar C, Clement K. Secretory type II phospholipase A2 is produced and secreted by epicardial adipose tissue and overexpressed in patients with coronary artery disease. *J Clin Endocrinol Metab* 2010;**95**:963–967.
25. Prifti E, Zucker JD, Clement K, Henegar C. FunNet: an integrative tool for exploring transcriptional interactions. *Bioinformatics* 2008;**24**:2636–2638.
26. Prifti E, Zucker JD, Clement K, Henegar C. Interactional and functional centrality in transcriptional co-expression networks. *Bioinformatics* 2010;**26**:3083–3089.
27. Henegar C, Tordjman J, Achard V, Lacasa D, Cremer I, Guerre-Millo M, Poitou C, Basdevant A, Stich V, Viguerie N, Langin D, Bedossa P, Zucker JD, Clement K. Adipose tissue transcriptomic signature highlights the pathological relevance of extracellular matrix in human obesity. *Genome Biol* 2008;**9**:R14.
28. Qatanani M, Tan Y, Dobrin R, Greenawalt DM, Hu G, Zhao W, Olefsky JM, Sears DD, Kaplan LM, Kemp DM. Inverse regulation of inflammation and mitochondrial function in adipose tissue defines extreme insulin sensitivity in morbidly obese patients. *Diabetes* 2013;**62**:855–863.
29. Wolfs MG, Rensen SS, Bruin-Van Dijk EJ, Verdam FJ, Greve JW, Sanjabi B, Bruinenberg M, Wijmenga C, van Haeften TW, Buurman WA, Franke L, Hofker MH. Co-expressed immune and metabolic genes in visceral and subcutaneous adipose tissue from severely obese individuals are associated with plasma HDL and glucose levels: a microarray study. *BMC Med Genomics* 2010;**3**:34.
30. Hirata Y, Tabata M, Kurobe H, Motoki T, Akaike M, Nishio C, Higashida M, Mikasa H, Nakaya Y, Takanashi S, Igarashi T, Kitagawa T, Sata M. Coronary atherosclerosis is associated with macrophage polarization in epicardial adipose tissue. *J Am Coll Cardiol* 2011;**58**:248–255.
31. Imoto-Tsubakimoto H, Takahashi T, Ueyama T, Ogata T, Adachi A, Nakanishi N, Mizushima K, Naito Y, Matsubara H. Serglycin is a novel adipocytokine highly expressed in epicardial adipose tissue. *Biochem Biophys Res Commun* 2013;**432**:105–110.
32. Park SU, Ahn DJ, Jeon HJ, Kwon TR, Lim HS, Choi BS, Baek KH, Bae H. Increase in the contents of ginsenosides in raw ginseng roots in response to exposure to 450 and 470 nm light from light-emitting diodes. *J Ginseng Res* 2012;**36**:198–204.
33. Divoux A, Tordjman J, Lacasa D, Veyrie N, Hugol D, Aissat A, Basdevant A, Guerre-Millo M, Poitou C, Zucker JD, Bedossa P, Clement K. Fibrosis in human adipose tissue: composition, distribution, and link with lipid metabolism and fat mass loss. *Diabetes* 2010;**59**:2817–2825.
34. Guauque-Olarte S, Gaudreault N, Piche ME, Fournier D, Mauriege P, Mathieu P, Bosse Y. The transcriptome of human epicardial, mediastinal and subcutaneous adipose tissues in men with coronary artery disease. *PLoS ONE* 2011;**6**:e19908.
35. Cousin B, Cinti S, Morroni M, Raimbault S, Ricquier D, Penicaud L, Casteilla L. Occurrence of brown adipocytes in rat white adipose tissue: molecular and morphological characterization. *J Cell Sci* 1992;**103**(Pt 4):931–942.
36. Sidossis L, Kajimura S. Brown and beige fat in humans: thermogenic adipocytes that control energy and glucose homeostasis. *J Clin Invest* 2015;**125**:478–486.
37. Wu J, Bostrom P, Sparks LM, Ye L, Choi JH, Giang AH, Khandekar M, Virtanen KA, Nuutila P, Schaart G, Huang K, Tu H, van Marken Lichtenbelt WD, Hoeks J, Enerback S, Schrauwen P, Spiegelman BM. Beige adipocytes are a distinct type of thermogenic fat cell in mouse and human. *Cell* 2012;**150**:366–376.
38. Jespersen NZ, Larsen TJ, Peijs L, Daugaard S, Homoe P, Loft A, de Jong J, Mathur N, Cannon B, Nedergaard J, Pedersen BK, Moller K, Scheele C. A classical brown adipose tissue mRNA signature partly overlaps with brite in the supraclavicular region of adult humans. *Cell Metab* 2013;**17**:798–805.
39. Nedergaard J, Cannon B. How brown is brown fat? It depends where you look. *Nat Med* 2013;**19**:540–541.
40. Wu J, Cohen P, Spiegelman BM. Adaptive thermogenesis in adipocytes: is beige the new brown? *Genes Dev* 2013;**27**:234–250.
41. Petrovic V, Buzadzic B, Korac A, Vasilijevic A, Jankovic A, Korac B. Free radical equilibrium in interscapular brown adipose tissue: relationship between metabolic profile and antioxidative defense. *Comp Biochem Physiol C Toxicol Pharmacol* 2006;**142**:60–65.
42. Bordicchia M, Liu D, Amri EZ, Ailhaud G, Dessi-Fulgheri P, Zhang C, Takahashi N, Sarzani R, Collins S. Cardiac natriuretic peptides act via p38 MAPK to induce the brown fat thermogenic program in mouse and human adipocytes. *J Clin Invest* 2012;**122**:1022–1036.
43. Tan BK, Adya R, Randeva HS. Omentin: a novel link between inflammation, diabesity, and cardiovascular disease. *Trends Cardiovasc Med* 2010;**20**:143–148.
44. Zhong X, Li X, Liu F, Tan H, Shang D. Omentin inhibits TNF-alpha-induced expression of adhesion molecules in endothelial cells via ERK/NF-kappaB pathway. *Biochem Biophys Res Commun* 2012;**425**:401–406.
45. Maruyama S, Shibata R, Kikuchi R, Izumiya Y, Rokutanda T, Araki S, Kataoka Y, Ohashi K, Daida H, Kihara S, Ogawa H, Murohara T, Ouchi N. Fat-derived factor omentin stimulates endothelial cell function and ischemia-induced revascularization via endothelial nitric oxide synthase-dependent mechanism. *J Biol Chem* 2012;**287**:408–417.
46. Yamawaki H, Kuramoto J, Kameshima S, Usui T, Okada M, Hara Y. Omentin, a novel adipocytokine inhibits TNF-induced vascular inflammation in human endothelial cells. *Biochem Biophys Res Commun* 2011;**408**:339–343.
47. Yamawaki H, Tsubaki N, Mukohda M, Okada M, Hara Y. Omentin, a novel adipokine, induces vasodilation in rat isolated blood vessels. *Biochem Biophys Res Commun* 2010;**393**:668–672.

48. de Souza Batista CM, Yang RZ, Lee MJ, Glynn NM, Yu DZ, Pray J, Ndubuizu K, Patil S, Schwartz A, Kligman M, Fried SK, Gong DW, Shuldiner AR, Pollin TI, McLenithan JC. Omentin plasma levels and gene expression are decreased in obesity. *Diabetes* 2007; **56**:1655–1661.
49. Pan HY, Guo L, Li Q. Changes of serum omentin-1 levels in normal subjects and in patients with impaired glucose regulation and with newly diagnosed and untreated type 2 diabetes. *Diabetes Res Clin Pract* 2010;**88**:29–33.
50. Fain JN, Sacks HS, Buehrer B, Bahouth SW, Garrett E, Wolf RY, Carter RA, Tichansky DS, Madan AK. Identification of omentin mRNA in human epicardial adipose tissue: comparison to omentin in subcutaneous, internal mammary artery periadventitial and visceral abdominal depots. *Int J Obes (Lond)* 2008;**32**:810–815.
51. Greulich S, Chen WJ, Maxhera B, Rijzewijk LJ, van der Meer RW, Jonker JT, Mueller H, de Wiza DH, Floerke RR, Smiris K, Lamb HJ, de Roos A, Bax JJ, Romijn JA, Smit JW, Akhyari P, Lichtenberg A, Eckel J, Diamant M, Ouwens DM. Cardioprotective properties of omentin-1 in type 2 diabetes: evidence from clinical and in vitro studies. *PLoS ONE* 2013;**8**:e59697.
52. Kim WS, Hsiao JH, Bhatia S, Glaros EN, Don AS, Tsuruoka S, Shannon Weickert C, Halliday GM. ABCA8 stimulates sphingomyelin production in oligodendrocytes. *Biochem J* 2013;**452**:401–410.
53. Wanders RJ, Visser WF, van Roermund CW, Kemp S, Waterham HR. The peroxisomal ABC transporter family. *Pflugers Arch* 2007;**453**:719–734.
54. Devlin CM, Leventhal AR, Kuriakose G, Schuchman EH, Williams KJ, Tabas I. Acid sphingomyelinase promotes lipoprotein retention within early atheromata and accelerates lesion progression. *Arterioscler Thromb Vasc Biol* 2008;**28**:1723–1730.
55. Hla T, Dannenberg AJ. Sphingolipid signaling in metabolic disorders. *Cell Metab* 2012; **16**:420–434.
56. Chami M, Gozuacik D, Lagorce D, Brini M, Falson P, Peaucellier G, Pinton P, Lecoeur H, Gougeon ML, le Maire M, Rizzuto R, Brechot C, Paterlini-Brechot P. SERCA1 truncated proteins unable to pump calcium reduce the endoplasmic reticulum calcium concentration and induce apoptosis. *J Cell Biol* 2001;**153**:1301–1314.
57. Weisser-Thomas J, Dieterich E, Janssen PM, Schmidt-Schweda S, Maier LS, Sumbilla C, Pieske B. Method-related effects of adenovirus-mediated LacZ and SERCA1 gene transfer on contractile behavior of cultured failing human cardiomyocytes. *J Pharmacol Toxicol Methods* 2005;**51**:91–103.
58. Perry SV. What is the role of tropomyosin in the regulation of muscle contraction? *J Muscle Res Cell Motil* 2003;**24**:593–596.
59. Gaborit B, Abdesselam I, Dutour A. Epicardial fat: more than just an 'epi' phenomenon? *Horm Metab Res* 2013;**45**:991–1001.